

Elsevier required licence: © <2021>. This manuscript version is made available under the CC-BY-NC-ND 4.0 license <http://creativecommons.org/licenses/by-nc-nd/4.0/>
The definitive publisher version is available online at <https://doi.org/10.1016/j.compgeo.2020.103960>

1 **On Numerical Simulation of Vertical Drains Using Linear**
2 **1-Dimensional Drain Elements**
3

4 **Mojtaba E. Kan**

5 *BSc (Hons), MSc, PhD (UNSW)*

6 Principal Engineer, Dams and Geotechnical, South Australian Water Corp., Australia

7 Formerly, Research Associate, Centre for Geomechanics and Railway Engineering, School of
8 Civil Engineering, Faculty of Engineering,

9 The University of Wollongong, Wollongong City, NSW 2522, Australia

10 Email: mojtaba@uow.edu.au
11

12 **Buddhima Indraratna**

13 *BSc (Hons., Lond.), MSc (Lond.), DIC, PhD (Alberta), FTSE, FIEAust., FASCE, FGS*

14 Distinguished Professor and Director, Transport Research Centre, University of Technology Sydney, NSW 2007;

15 Email: buddhima.indraratna@uts.edu.au, Ph: +61 400 213 046
16

17 **Cholachat Rujikiatkamjorn**

18 *BEng (Hons), MEng (AIT), PhD*

19 Professor, School of Civil & Environmental Engineering, University of Technology Sydney, NSW 2007

20 Email: cholachat.rujikiatkamjorn@uts.edu.au
21

22 Prepared for submission to **Computers and Geotechnics**

23 No. of Words (without abstract and references): **2800** No of Figures: **10**, No of Tables: **2**
24
25
26
27

28 On Numerical Simulation of Vertical Drains Using Linear
29 1-Dimensional Drain Elements

30 **Mojtaba E. Kan, Buddhima Indraratna, and Cholachat Rujikiatkamjorn**

31
32 **Abstract**

33
34 This Technical Note addresses an issue of vertical drains simulation using linear drain elements
35 for radial consolidation. A new method is proposed which enables the application of linear drain
36 elements while maintaining acceptable accuracy. The robustness of the proposed method is
37 examined satisfactorily through the simulation of a unit cell representing a single drain and the
38 application of multi-drain condition for the Ballina Embankment considering both elastic and
39 elasto-plastic soil domains.

40 The proposed model shows that the settlement and excess pore pressure predictions are almost the
41 same as those determined for the ideal. The effectiveness of this method is also demonstrated
42 through the reduction of the numerical convergence time for both unit cell and multi-drain
43 conditions.

44
45 **Keywords:** Vertical drains, Consolidation, Drain, Drain elements, Smear Zone, Numerical
46 simulation

50 **1 Introduction**

51 The behaviour of soft clay stabilized with prefabricated vertical drains (PVDs) has remained
52 difficult to predict accurately, although many numerical modelling tools have become available.
53 The classical radial consolidation theory using a unit cell was well documented in Barron (1948)
54 and later was extended by Hansbo (1981). The unit cell analysis however fails to predict the
55 settlement and lateral displacement far from the embankment centreline where the assumption of
56 zero lateral displacements is not valid anymore. To analyse a multi-drain system, most finite
57 element analyses on embankments are usually conducted based on the plane strain assumption
58 given the significantly longer dimension of the embankment compared to its width, although the
59 consolidation around a vertical drain is axisymmetric (3D). In large projects, there are thousands
60 of PVDs, and a comprehensive 3D analysis to capture all these individual unit cells is cumbersome
61 and often impractical. The multidrain analysis, therefore, is essential to incorporate the effect of
62 variations in lateral confinement along the embankment width. Following the initial developments
63 in this field (e.g. Cheung et al., 1991, Hird et al., 1992, Chai and Carter 2011, Chai et al. 2013),
64 Indraratna and Redana (1997, 2000) extended the conversion technique to include the effects of
65 smear zone, a zone of soil around the drain with lower permeability due to the installation of the
66 vertical drain. By employing a realistic equivalent plane strain analysis for PVDs, the need for
67 cumbersome 3D axisymmetric analysis for each drain can be avoided as further explained by
68 Rujikiatkamjorn et al. (2008).

69 Although a significant amount of research works have been devoted to model smear zone, there
70 are limited studies about employing various forms of drain elements in numerical simulation of
71 multidrain systems (e.g. in Zhu and Yin, 2000, Indraratna et al., 2003, Ngo et al. 2020). Nowadays,
72 however, few numerical simulation packages such as PLAXIS (Brinkgreve et al., 2015) have

73 one-dimensional (1D) drain element using a zero-thickness line. In FLAC (Itasca Consulting
74 Group Inc., 2008), the drain shall be simulated using assigned pore water pressure on particular
75 nodes along the drain and therefore the width of the drain cannot be simulated directly in
76 simulations (e.g. in Chai et al. 2013; Parsa-Pajouh et al., 2014; Nguyen et al. 2018).

77 In this Note, a novel approach is introduced by which the drain elements can be appropriately used
78 in the simulation of PVDs and their surrounding smear zone. In this approach, the effect of drain
79 size in numerical modelling is incorporated by specifying an adjusted size of the smear zone based
80 on given drain size and soil permeability.

81 **2 Proposed simulation scheme**

82 Analytical modelling of radial consolidation involves a cylinder of soil around a single vertical
83 drain (Figure 1a). Figure 1(b) shows a unit cell with an effective diameter of d_e , surrounding a
84 single drain with diameter of d_w and smear zone with a diameter of d_s . The horizontal permeability
85 coefficients of the undisturbed and smear zone are denoted as k_h and k_s , respectively. Under a
86 plane strain analysis (Figure 1c), the equivalent horizontal permeability can be calculated using
87 the conversion technique described by Indraratna and Redana (2000):

$$88 \quad \frac{k_{hp}}{k_h} = \frac{2/3}{\ln(n) - 0.75} \quad (1)$$

89 where $n = d_e / d_w$. The converted coefficients of permeability in plane strain model for undisturbed
90 and smear zone are k_{hp} and k_{sp} , respectively. The equivalent permeability of the smear zone under
91 plane strain condition can be calculated from:

92
$$\frac{k_{sp}}{k_{hp}} = \frac{\beta}{\frac{k_{hp}}{k_h} \left[\ln(n) + \frac{k_h}{k_s} \ln(s) - 0.75 \right] - \alpha} \quad (2)$$

93 where $s = d_s / d_w$, α and β can be calculated from:

94
$$\alpha = \frac{2}{3} \frac{(n-s)^3}{n^2(n-1)}, \beta = \frac{2(s-1)}{n^2(n-1)} \left[n(n-s-1) + \frac{1}{3}(s^2 + s + 1) \right] \quad (3)$$

95 A plane strain unit cell shown in Figure 1 can be conveniently simulated using linear 1D drain
 96 elements. To correctly simulate the drain with its thickness (Figure 2a), the drain should be
 97 represented by 2D elements sandwiched by 1D drain elements on both sides (Case I). In this
 98 approach, owing to the relatively small thickness of the drain compared with the surrounding soil,
 99 an extremely small mesh size inside the drain is required.

100 To avoid the above situation, one may decide to simulate the drain with a single drain element
 101 (Case II), shown in Figure 2(b). In this case, however, the actual size of the drain is ignored and
 102 therefore the size of the smear zone is larger than those measured in the field (Indraratna et al.,
 103 2014) or laboratory conditions (e.g. Rujikiatkamjorn et al., 2013).

104 One possible approach to solve this problem is to introduce the smear zone with a permeability of
 105 k' , and width of $2b'$ (Case III), (Figure 2c) by taking into account the vertical drain's equivalent
 106 thickness.

107 If flow continuity is satisfied, an equivalent permeability of the undisturbed-smear soil systems
 108 in each case can be described below.

109 For Case I (Figure 2a):

110
$$\frac{B}{k} = \frac{b_w}{k_w} + \frac{b_s - b_w}{k_{sp}} + \frac{B - b_s}{k_{hp}} \quad (4)$$

111 For Case II (Figure 2b):

$$112 \quad \frac{B}{\bar{k}} = \frac{b'}{k'} + \frac{B-b'}{k_{hp}} \quad (5)$$

113 where \bar{k} is the average equivalent permeability of the unit cell. As the permeability of the vertical
114 drain is very high (Indraratna and Chu, 2005), the term b_w/k_w is much smaller than two other
115 terms and then equation (4) can be re-written as:

$$116 \quad \frac{B}{\bar{k}} = \frac{b_s - b_w}{k_{sp}} + \frac{B - b_s}{k_{hp}} \quad (6)$$

117 The right-hand side of Equations (5) and (6) should be equal, which yields:

$$118 \quad b' = b_s \frac{k_{hp} - k_{sp}}{k_{hp} - k'} - \frac{b_w k_{hp}}{k_{sp} (k_{hp} - k')} \quad (7)$$

119 The permeability of the converted smear zone however can be assumed the same as the original
120 smear zone, i.e. $k' = k_{sp}$, therefore, Equation (7) can be simplified to have:

$$121 \quad b' = b_s - \frac{b_w}{1 - k_{sp}/k_{hp}} \quad (8)$$

122 By defining $s' = b' / b_w$, Equation (8) can be written as:

$$123 \quad s' = s - \frac{1}{1 - k_{sp}/k_{hp}} \quad (9)$$

124 Similar to the plane-strain condition, it can be shown that the same adjusted size of the smear zone
125 is required to use (1D) drain elements in the simulation of an axisymmetric unit cell. The

126 corresponding diameter of the adjusted smear zone for axisymmetric condition, d' , and the smear
127 size ratio, $s' = d' / d_w$, can be calculated using the following equations:

$$128 \quad d' = d_s - \frac{d_w}{1 - k_s/k_h} \quad \text{and} \quad s' = s - \frac{1}{1 - k_s/k_h} \quad (10)$$

129 Parsa-Pajouh et al. (2014) showed that the value of s may vary from 1.6 to 7 times and the range
130 of the undisturbed to smeared permeability ratios (k_s / k_h) might be 0.1–0.8. The variation of s'
131 with s for a range of possible k_s / k_h values and based on Equation (10) is shown in Figure 3.

132 **3 Verification of the Approach**

133 Indraratna et al. (2005) reported the results of analytical and numerical modelling to predict the
134 consolidation behaviour of soft estuarine Sydney clay using a physical model. Similar to their
135 study, a 0.95 m high, 0.45m diameter unit cell was simulated with the drain and surrounding smear
136 zone diameter of 50 and 170 mm, respectively. The triangular elements (six-node quadratic
137 displacement and linear pore pressure) were used in the finite element discretization throughout
138 the Note (Figure 4a). The drain was simulated using a linear drain element. Simulations were
139 performed using PLAXIS 2D (Brinkgreve et al., 2015) were divided into three cases:

- 140 • Case I: vertical drain was simulated using ultra-fine mesh in axisymmetric condition
141 (Figure 4b). A total of 1095 elements were used to model only half of the problem due to
142 the symmetric conditions.
- 143 • Case II: vertical drain was simulated using 1D drain elements (Figure 4c) with a total of
144 1716 elements.

- 145 • Case III: vertical drain was simulated using 1D drain elements, with a converted size of the
146 smear zone based on the size of the drain and normalized permeability of the smear zone,
147 (Figure 4d). A total of 1540 elements were used in this case.

148 The soil behaviour was assumed to be linear elastic with $m_v=0.001 \text{ m}^2/\text{kN}$ and the zero lateral
149 displacements were imposed (Poisson's ratio = 0) for the unit cell. The horizontal undisturbed soil
150 permeability (k_h) was taken as 10^{-10} m/s , and the ratio of the undisturbed permeability to the
151 smear zone permeability (k_h/k_s) was assumed to be 3.0 (Indraratna and Redana, 2000).
152 Conversion of the permeability values for plane-strain simulations in Cases (II) and (III) was
153 performed using Equations (1) and (2). In Case (III) the size of the smear zone was adjusted using
154 Equation (8). The converted size of the smear zone after application of the proposed scheme was
155 106 mm which compared with the original size of 170 mm shows a 37% reduction in size. A
156 summary of the required conversion calculations is given in Table 1. By the size of the smear zone
157 in Case (III), it is expected that the effect of drain size would be incorporated.

158 In all cases, the top, bottom, and outer boundaries were set as impermeable to allow only horizontal
159 flow. After establishing the at-rest in-situ stresses, the drain elements were activated and then a
160 surcharge load of 50 kPa was applied on top of the cell. To capture the equal-strain condition, rigid
161 elements were used at the top of the soil surface where only vertical displacement was allowed to
162 prevent any rotation. The fully implicit time-marching scheme with a default error tolerance of 1%
163 was adopted to ensure adequate and swift convergence throughout the Note.

164 The normalized excess pore water pressure in the numerical simulations was calculated using the
165 average values at observation points. The presented analytical solution is based on the radial
166 consolidation equation by Hansbo, (1981) where the coefficient of consolidation in a radial

167 direction, equal to $0.315 \text{ m}^2/\text{year}$. It can be seen in Figure 5(a) that the results of the numerical
168 simulations in Case I are very close to those of the analytical solution, as expected. While the
169 simulated curve for excess pore pressure in Case II deviates from the analytical results especially
170 after 10 days, the proposed scheme in Case III shows similar results compared with the analytical
171 model. The effect of different numerical schemes can be clearly shown using the percentage error
172 in the calculation of the excess pore water pressure (Figure 5b). It can be seen that in Case II the
173 error in the calculation of excess pore water pressure can be as high as 8% at 150 days, while by
174 application of the proposed method (Case III) the error decreases to be less than 4%. Note that the
175 application of the numerical model may introduce an inherent error that is depicted in the
176 simulation of Case I and might be as high as 2%. If the inherent error is subtracted from the
177 numerical simulation results, the net maximum error in the proposed model is less than 2% which
178 is acceptable for most practical applications.

179 **4 Application to a case study under multidrain simulation**

180 In the unit cell, simulation of the radial consolidation using Case 1 seems to be the most accurate
181 numerical scheme among the 3 proposed schemes. In multidrain problems however, it might be
182 very time-consuming to use a simulation scheme based on Case I due to the excessive number of
183 small size elements to simulate the drain. In contrast, the application of the proposed simulation
184 scheme based on Case III would provide enough accuracy very close to the ideal condition and
185 without the need for time-consuming simulation.

186 To demonstrate the performance of each scheme, two multidrain problems were analysed, one
187 based on elastic behaviour attributed to Sydney soft clay, and the other one based on an
188 elastoplastic condition corresponding to the plastic Ballina clay.

189 4.1 Multidrain system in elastic condition

190 For relatively small embankment, a multidrain system consisting of 5 PVDs, 10 m deep with 1 m
191 spacing, was considered with the same properties of Sydney soft clay described in the previous
192 section.

193 Simulations were performed in two cases:

- 194 • Case A: PVDs were simulated similar to Case I under plane strain condition (Figure 6a),
195 with a total of 9606 soil elements
- 196 • Case B: PVDs were simulated similar to Case III with the converted size of the smear zone
197 (Figure 6b) with a total of 5804 soil elements.

198 Conversion of the permeability under plane strain condition is performed using equations (1) and
199 (2). In Case B the size of the smear zone is adjusted using the proposed scheme which resulted in
200 a 22% reduction of smear zone width. All required parameters based on each conversion scheme
201 are summarized in Table 1.

202 The in-situ stresses were established in the model using $k_o = 1$ and then the drains were activated
203 after 5 days. A surcharge load of 50 kPa was applied then on top of the model in a width of 5 m
204 from the centreline.

205 Figure 7 shows the rate of consolidation calculated based on the ratio of time-dependent settlement
206 at point A (see Figure 6). It can be seen that both cases show the same rate of consolidation at the
207 centreline. It can be seen that for both points B and C (see Figure 6), Case B provides the excess
208 pore water pressure predictions almost identical to those of Case A.

209 4.2 Multidrain system in elastoplastic condition using soft soil model

210 A trial embankment was constructed at the southern approach of the upgraded highway to
211 Emigrant Creek, north of Ballina town NSW, Australia, to study the effectiveness of different
212 ground improvement techniques. A section of this embankment, namely Section-A, was selected,
213 in which the circular-shaped PVDs with surcharge only was used for ground stabilization (Kelly
214 and Wong, 2009). In this section of the embankment, the soft clay layer was 7 m in depth, underlain
215 by stiff Pleistocene silty clay which is assumed unaffected during the ground improvement. The
216 PVDs were 34 mm in diameter, installed at a spacing of 1.0 m in a square pattern (Indraratna et
217 al., 2012). The embankment height was raised to 5.4 m in multiple stages in 1200 days, using fill
218 materials with an average unit weight of 20 kN/m^3 (Parsa-Pajouh et al., 2014).

219 Only half of the embankment is shown here owing to the symmetric geometry of the system
220 (Figure 8a). Two cases were considered for simulations:

- 221 • Case C: An ideal model with two drain elements per each PVD and ultra-fine mesh inside
222 the drain (Figure 8b), with a total number of 13800 soil elements
- 223 • Case D: The proposed model with the converted size of the smear zone (Figure 8c) with a
224 total number of 4143 soil elements.

225 As summarized in Table 1, the permeability for the plane strain condition was calculated using
226 Equations (1) and (2). The size of the smear zone was adjusted in Case D, using the proposed
227 scheme and consequently, the width of the smear zone was reduced by 12%.

228 The required material parameters for Soft Soil model were adopted from relevant literature, mainly
229 from Indraratna et al. (2012), as listed in Table 2. The staged construction (Figure 9) was simulated
230 as follows (a) at-rest equilibrium condition, (b) the placement of working platform (0.6 m high),

231 (c) rest period for installation of PVDs, (d) placement of sand blanket (0.7 m thick), (e) rest period
232 for installation of instruments, and (f) raising the embankment to the ultimate height (7m). In each
233 stage, the corresponding surcharge load was applied on top of the model and the lateral batter of
234 the embankment was simply simulated using a trapezoidal load distribution (Figure 8a).

235 Figure 9 shows the results of simulations compared with the measured surface settlement at SP1,
236 at the embankment centreline. It can be seen that both cases show the same rate of settlement at
237 the centreline which is fairly close to the field measurements. The proposed model in Case D,
238 therefore, shows the settlement predictions almost the same as those of Case C with the ideal
239 condition but highly intense mesh. Although the validation using physical model and case studies
240 was conducted, further validation from more studies can enhance clarity and confidence in using
241 this approach.

242 **4.3 Effectiveness in saving the CPU time**

243 The benefits of the proposed scheme however can be further highlighted if the number of elements
244 and the time of CPU for simulation are taken into account.

245 For the problem of the multidrain system in Sydney clay with a drain width of 50 mm, it was
246 shown that the application of the proposed model reduced the number of elements by 40%, from
247 9606 elements in the ideal case (Case A) to 5804 in proposed case (Case B). In the problem of
248 Ballina Bypass embankment with smaller 34 mm diameter drains, the number of elements reduced
249 from 13800 in the ideal case (Case C) to 4143 in the proposed case (Case D), which shows a
250 significant 70% reduction in the number of elements. This comparison shows that as the size of
251 the drain in the prototype problem decreases, more intense mesh is necessary to simulate the model

252 in Case I, and therefore the benefits of the proposed scheme (Case III) to reduce the number of
253 elements and consequently the CPU time are more pronounced.

254 From the perspective of the calculation time, the effect of constitutive model complexity should
255 also be taken into account. The required processor times for simulation of the two multidrain
256 systems are compared in Figure 10, where on the horizontal axis, the term Elastic denotes the
257 Sydney clay problem, and the term Elastoplastic is used to show the Ballina Bypass problem. The
258 CPU times are normalized for the ideal conditions in each problem and the simulations were
259 performed using a PC with 3.6 GHz Intel Xenon CPU and 32 GB RAM. It can be seen that using
260 the proposed scheme reduced the CPU time by 50-70%.

261 **5 Conclusions**

262 An alternative simulation scheme was proposed where the effect of the drain size could be
263 converted to an equivalent reduction in the size of the smear zone of the soil surrounding the drain.
264 The robustness of the proposed method was demonstrated using both single drain and multi-drain
265 systems, in comparison to an ideal or perfect drain simulation. It was shown that in both single and
266 multi-drain systems, the proposed method can predict the behaviour of the soil-drain system
267 accurately with insignificant deviation from the ideal simulation. It was shown that the efficiency
268 of the simulation can be significantly improved by the application of the proposed method, and
269 CPU time saving of 50-70% was observed in two multi-drain problems discussed within the scope
270 of this Note.

271 **6 Acknowledgment**

272 This research has been funded under the Australian Research Council (ARC) Linkage scheme
273 (LP140100065) as a collaboration among the Universities of Wollongong and Newcastle in
274 Australia and Imperial College of Science, Technology, and Medicine, University of London, UK.
275 The authors acknowledge the support of the industry partners Menard-Bachy, Coffey Geotechnics,
276 Douglas Partners, the National Jute Board of India, and Soilwicks Pty Ltd.

277 **7 Data Availability Statement**

278 Some or all data, models, or code that support the findings of this study are available from the
279 corresponding author upon reasonable request.

280

281 **8 References**

- 282 Barron, R. A. 1948. Consolidation of fine-grained soils by drain wells. *Transactions of American Society*
283 *of Civil Engineers, Paper No. 2346*, 113, 718–742.
- 284 Brinkgreve, R., Kumarswamy, S. and Swolfs, W. (eds.) 2015. *PLAXIS 2D 2015, User's Manual*,
285 Netherlands: Plaxis bv.
- 286 Chai, J.C. and Carter, J.P. 2011. *Deformation Analysis in Soft Ground Improvement*, Springer, Berlin.
- 287 Chai, J.C., Bergado, D.T, Shen, S.L. 2013. Modelling prefabricated vertical drain improved ground in
288 plane strain analysis. *Ground Improv.*, 166 (G12), pp. 65-77.
- 289 Cheung, Y., Lee, P. and Xie, K. 1991. Some remarks on two and three dimensional consolidation analysis
290 of sand-drained ground. *Computers and Geotechnics*, 12, 73-87.
- 291 Hansbo, S. 1981. Consolidation of fine-grained soils by prefabricated drains. *Proc. of 10th ICSMFE, 1981*,
292 3, 677-682.
- 293 Hird, C., Pyrah, I. and Russel, D. 1992. Finite element modelling of vertical drains beneath embankments
294 on soft ground. *Geotechnique*, 42, 499-511.
- 295 Indraratna, B., Bamunawita, C., Redana, I. and McIntosh, G. 2003. Modelling of prefabricated vertical
296 drains in soft clay and evaluation of their effectiveness in practice.
- 297 Indraratna, B. and Chu, J. 2005. *Ground Improvement—Case Histories*, London, UK, Elsevier.

298 Indraratna, B., Perera, D., Rujikiatkamjorn, C. and Kelly, R. 2014. Soil disturbance analysis due to vertical
299 drain installation. *Proceedings of the Institution of Civil Engineers - Geotechnical Engineering*,
300 168, 236-246.

301 Indraratna, B. and Redana, I. 1997. Plane-strain modeling of smear effects associated with vertical drains.
302 *Journal of Geotechnical and Geoenvironmental Engineering*, 123, 474-478.

303 Indraratna, B. and Redana, I. 2000. Numerical modeling of vertical drains with smear and well resistance
304 installed in soft clay. *Canadian Geotechnical Journal*, 37, 132-145.

305 Indraratna, B., Rujikiatkamjorn, C., Kelly, R. and Buys, H. 2012. Soft soil foundation improved by vacuum
306 and surcharge loading. *Proceedings of the ICE-Ground Improvement*, 165, 87-96.

307 Indraratna, B., Rujikiatkamjorn, C. and Sathananthan, I. 2005. Analytical and numerical solutions for a
308 single vertical drain including the effects of vacuum preloading. *Canadian Geotechnical Journal*,
309 42, 994-1014.

310 Itasca Consulting Group Inc. 2008. *FLAC-Fast Lagrangian Analysis of Continua, Ver. 6.0*, Minneapolis,
311 MN (USA).

312 Kelly, R. and Wong, P. 2009. An embankment constructed using vacuum consolidation. *Australian*
313 *Geomechanics*, 44, 55.

314 Parsa-Pajouh, A., Fatahi, B., Vincent, P. and Khabbaz, H. 2014. Trial Embankment Analysis to Predict
315 Smear Zone Characteristics Induced by Prefabricated Vertical Drain Installation. *Geotechnical and*
316 *Geological Engineering*, 32, 1187-1210.

317 Ngo, D.H. Horpibulsuk, S. Suddeepong, A. Hoy, M. Udomchai, A. Doncommul, P. Arulrajah A. 2020.
318 Consolidation behavior of dredged ultra-soft soil improved with prefabricated vertical drain at the
319 Mae Moh mine, Thailand. *Geotext. Geomembranes*, 48 pp. 561-571.

320 Nguyen, T. T., Indraratna, B. & Rujikiatkamjorn, C. 2018. A Numerical Approach to Model Biodegradable
321 Vertical Drains. *Environmental Geotechnics*, Online First 1-9.

322 Rujikiatkamjorn C., Indraratna, B. and Chu, J. 2008. 2D and 3D Numerical Modeling of Combined
323 Surcharge and Vacuum Preloading with Vertical Drains. *Intl. J of Geomechanics*, ASCE, 8(2), 144-
324 156.

325 Rujikiatkamjorn, C., Ardana, M., Indraratna, B. and Leroueil, S. 2013. Conceptual model describing smear
326 zone caused by mandrel action. *Géotechnique*, 63, 1377.

327 Zhu, G. and Yin, J.-H. 2000. Finite element consolidation analysis of soils with vertical drain. *International*
328 *Journal for Numerical and Analytical Methods in Geomechanics*, 24, 337-366.

329

330

331

332

Table 1: Conversion of permeability and size of smear zone for numerical models

Problem	$d_w = 2b_w$ (mm)	$d_s = 2b_s$ (mm)	$d_e = 2B$ (mm)	k_h (m/s)	$\frac{k_h}{k_s}$	n	s	α	β	$\frac{k_{hp}}{k_h}$	$\frac{k_{sp}}{k_{hp}}$	$d' = 2b'$ (mm)
Unit cell in Sydney soft clay	50	170	450	10^{-10}	3	9	3.4	0.181	0.346	0.461	0.214	106
Multidrain in Sydney soft clay	50	300	1000	10^{-10}	3	20	6	0.241	0.631	0.297	0.242	234
Multidrain in Ballina plastic clay	34	570	1000	10^{-9}	1.7	29	17	0.054	0.568	0.253	0.521	500

334

335

336

337

338

339

340

341

342

343

344

345

346

347

348

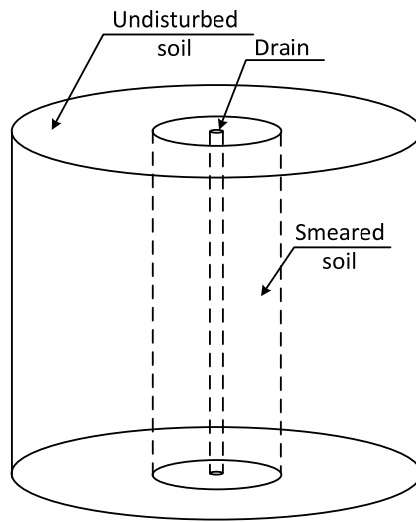
349

350

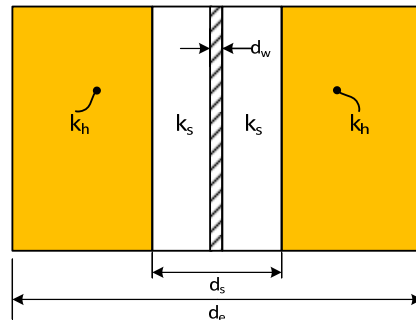
Table 2: Material parameters for Ballina soft clay in Soft Soil model

C_c	C_s	p'_c (kPa)	γ (kN/m ³)	e_o	K_o	c' (kPa)	ϕ'^o	k_h (m/s)	k_v (m/s)
1.31	0.14	20	14.5	2.9	0.75	5	25	10^{-9}	8×10^{-10}

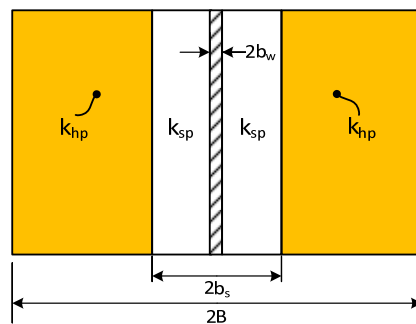
C_c : Compression index, in $e - \log \sigma'$ plane, C_s : Swelling index in $e - \log \sigma'$ plane, p'_c : pre-consolidation pressure, γ : Saturated unit weight, e_o : Initial void ratio, K_o : Coefficient of lateral pressure at-rest, c' : Drained cohesion, ϕ' : Drained friction angle, k_h and k_v : Coefficients of permeability in horizontal and vertical directions



(a)



(b)



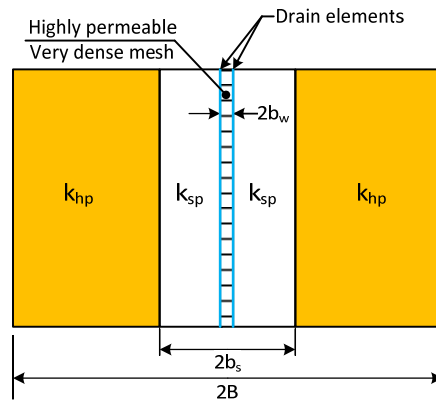
(c)

353

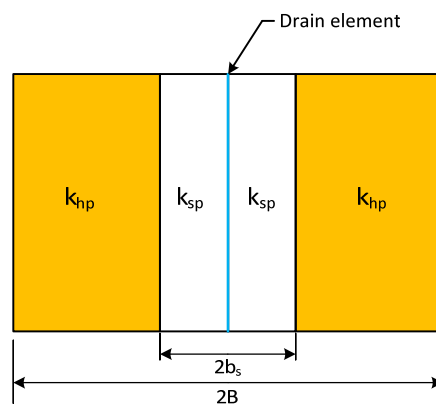
354

355

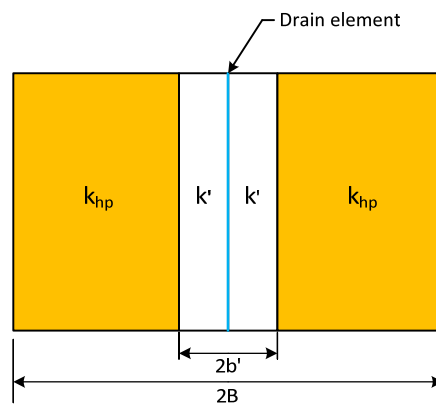
Figure 1: (a) A single drain and surrounding disturbed and undisturbed soils, (b) Unit cell of a drain-soil system in axisymmetric conditions, and (c) Converted unit cell in plane strain conditions



(a)



(b)



(c)

356

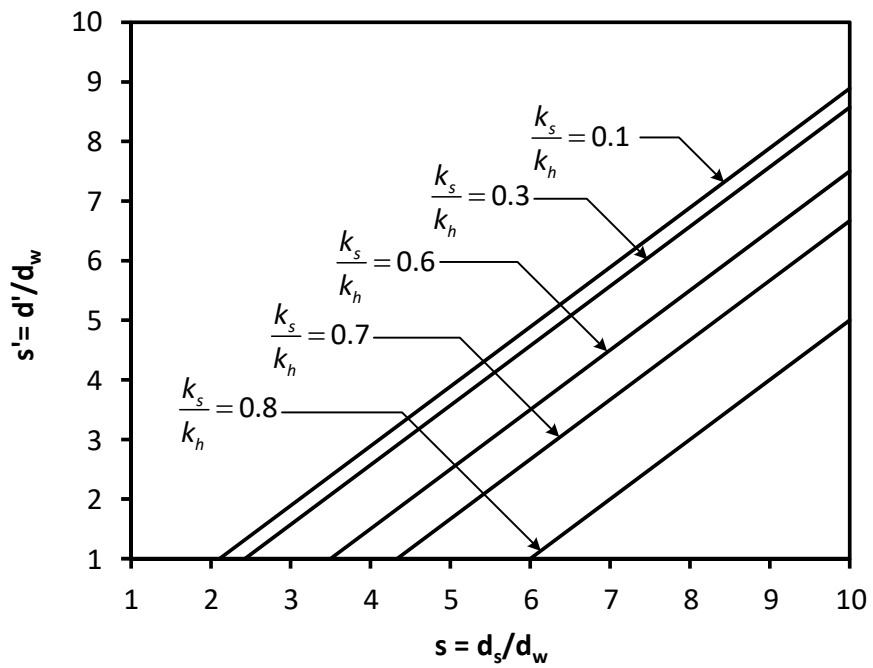
357

358

359

360

Figure 2: Simulation of plane-strain unit cell using linear drain elements using: (a) ultra-fine elements inside the drain (b) drain elements ignoring the effect of drain size, and (c) proposed scheme using converted size of the smear zone



361

362

Figure 3: Variation of s' with s for a range of smear zone permeability ratios

363

364

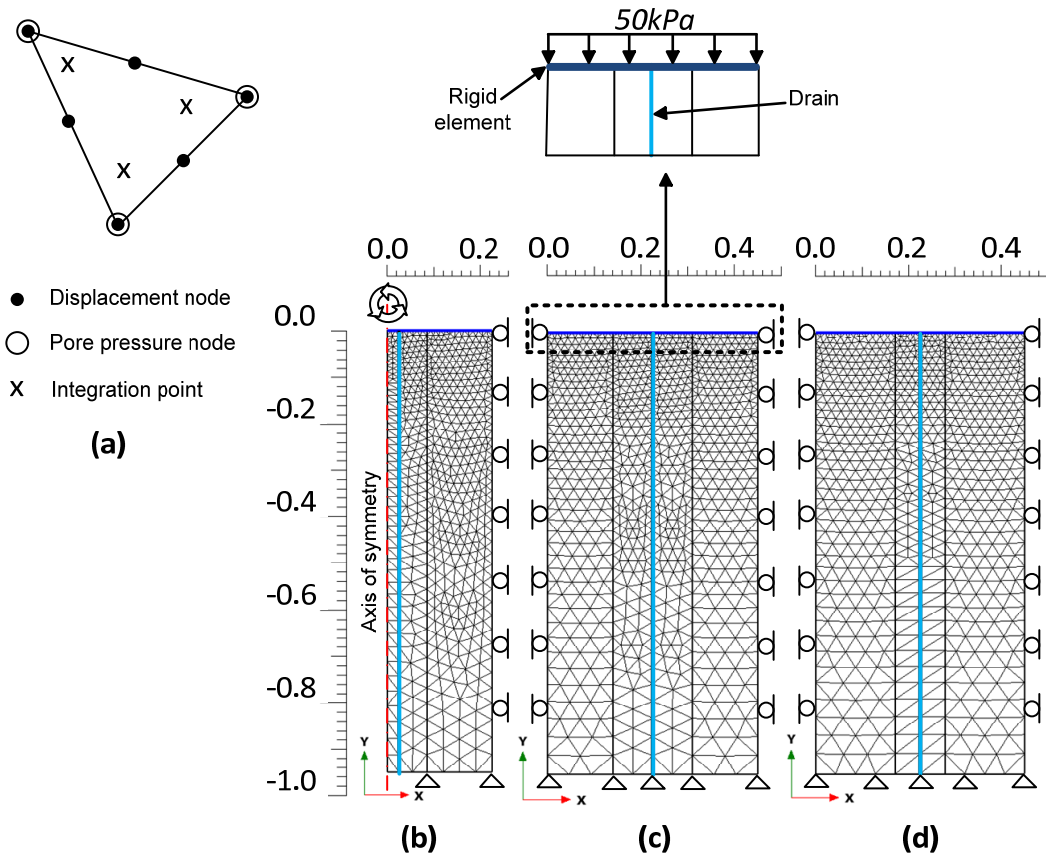
365

366

367

368

369



370

371 **Figure 4: Finite element discretization for unit cell: (a) nodes and integration points for a single 6-**

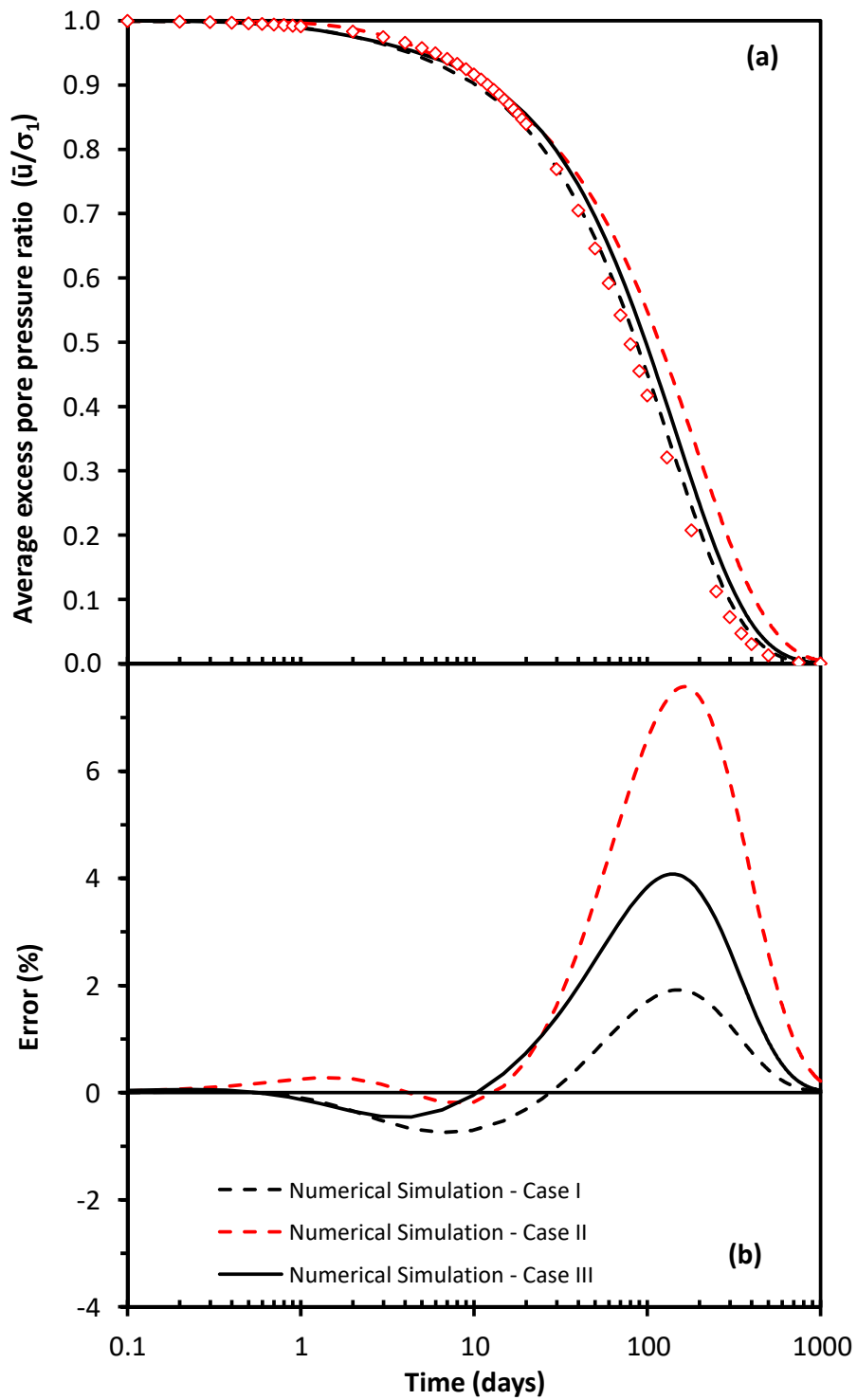
372 **node element; (b), (c), and (d) mesh discretization and boundary conditions for Case (I), Case (II),**

373 **and Case (III), respectively.**

374

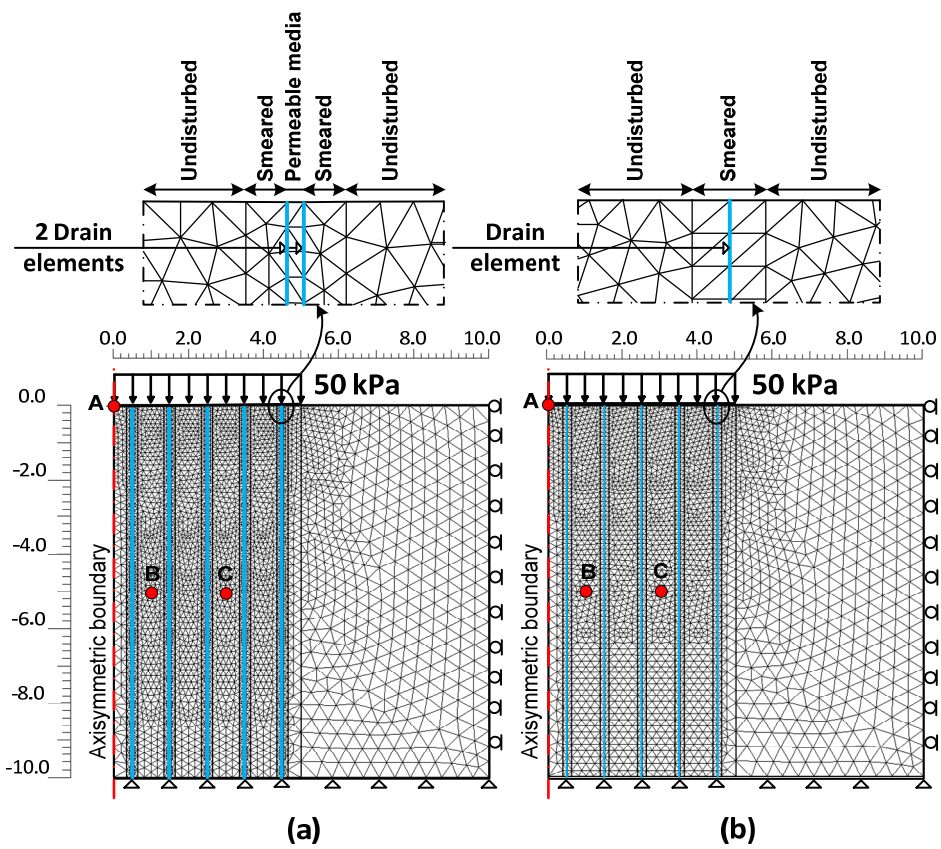
375

376



377
 378
 379
 380

Figure 5: Consolidation responses using different numerical schemes: (a) average excess pore pressure curve, and (b) error in calculation of average excess pore pressure in numerical models with respect to analytical solution



381

382

Figure 6: Mesh, boundary conditions and observation points of a multidrain problem: (a) Ideal simulation using two drain elements and a permeable media in between, and (b) Proposed model using single drain element and adjusted size of smear zone

384

385

386

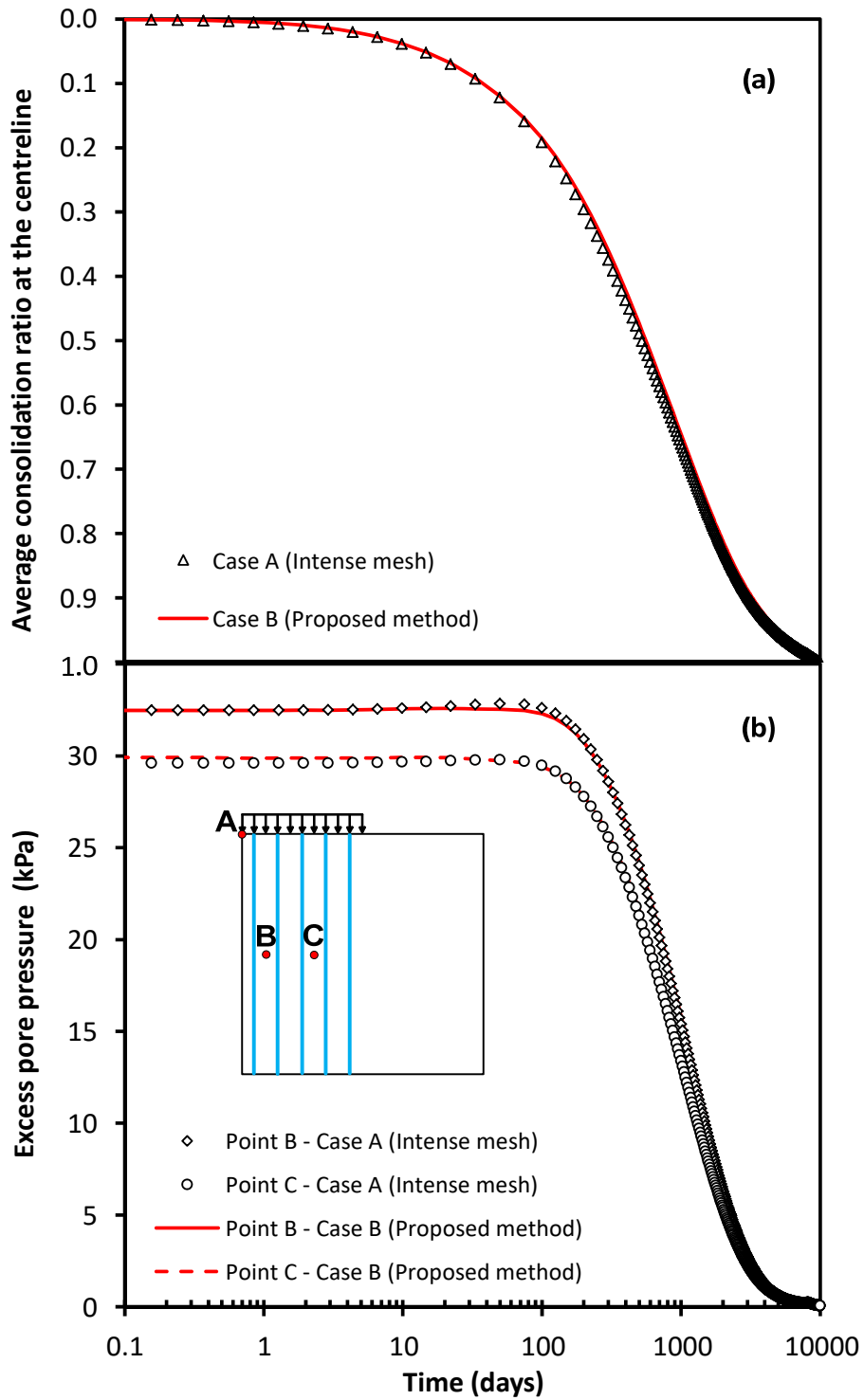
387

388

389

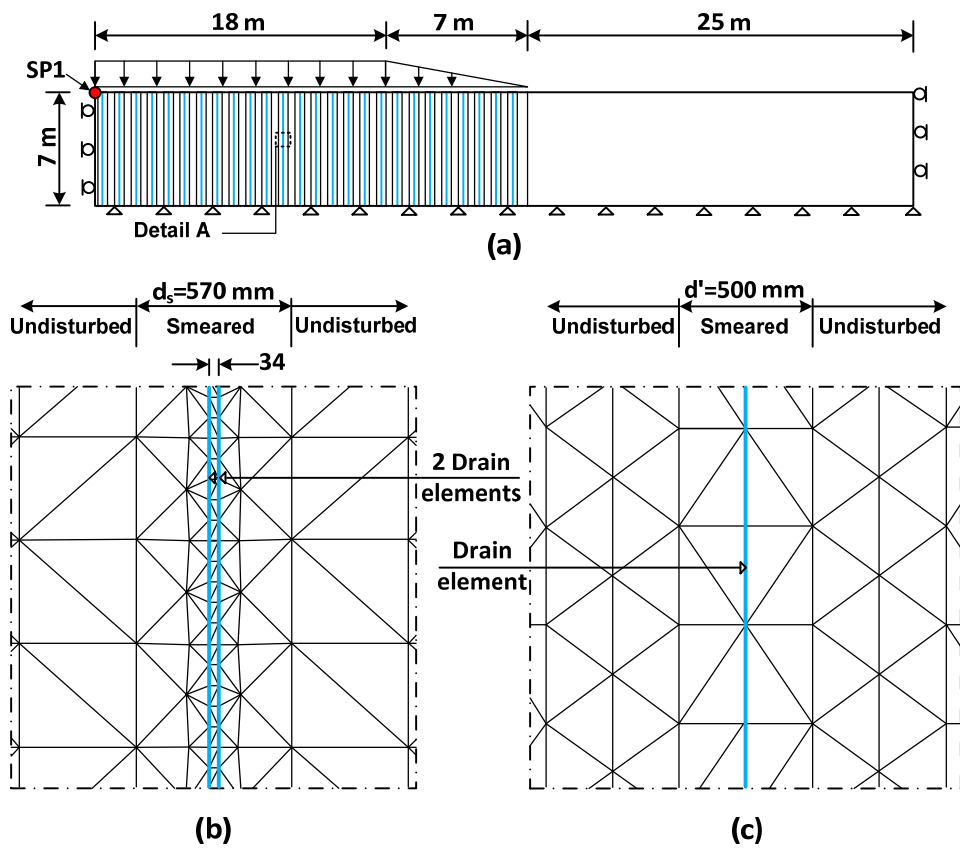
390

391



392
 393
 394
 395

Figure 7: Consolidation responses for multidrain analysis: (a) average consolidation ratio at the model centerline, and (b) excess pore water pressure at points B and C



396

397 **Figure 8: (a) Geometry and boundary conditions of multidrain system in Ballina soft clay, (b) Case**

398 **(I): ideal mesh using two drain elements and a permeable media in between, and (c) Case (II): a**

399 **proposed model using single drain element and adjusted size of smear zone**

400

401

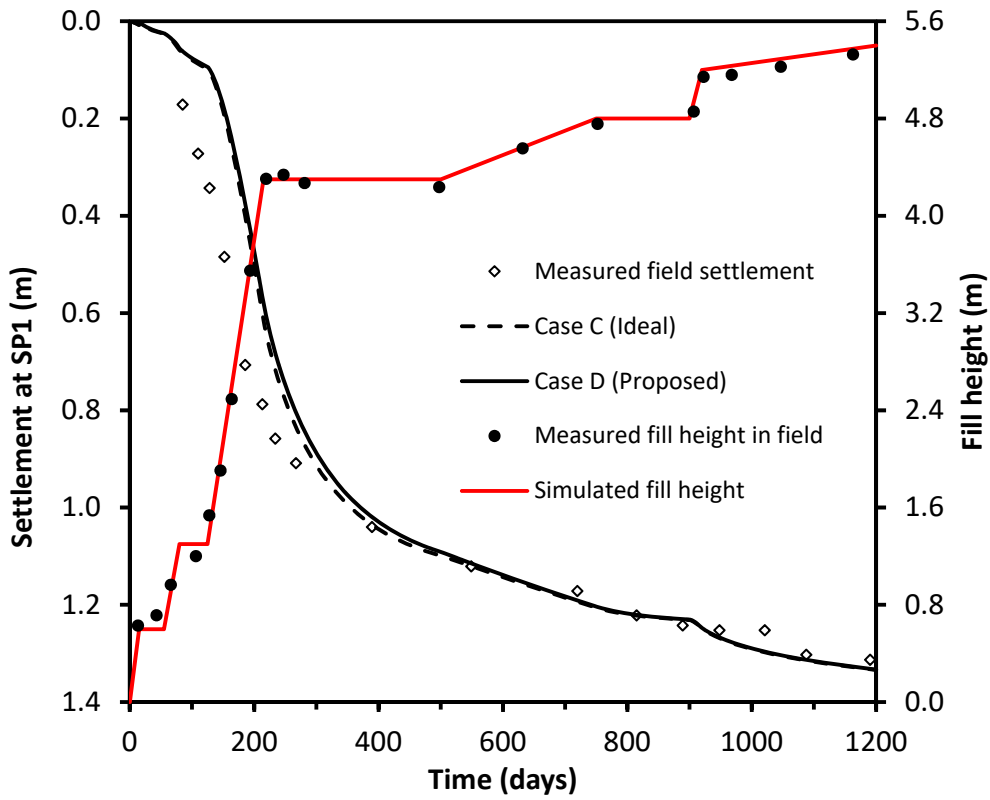
402

403

404

405

406



407
408

409

Figure 9: Simulation of Ballina Bypass Section-A trial embankment, loading history, and settlement at the embankment centerline

410

411

412

413

414

415

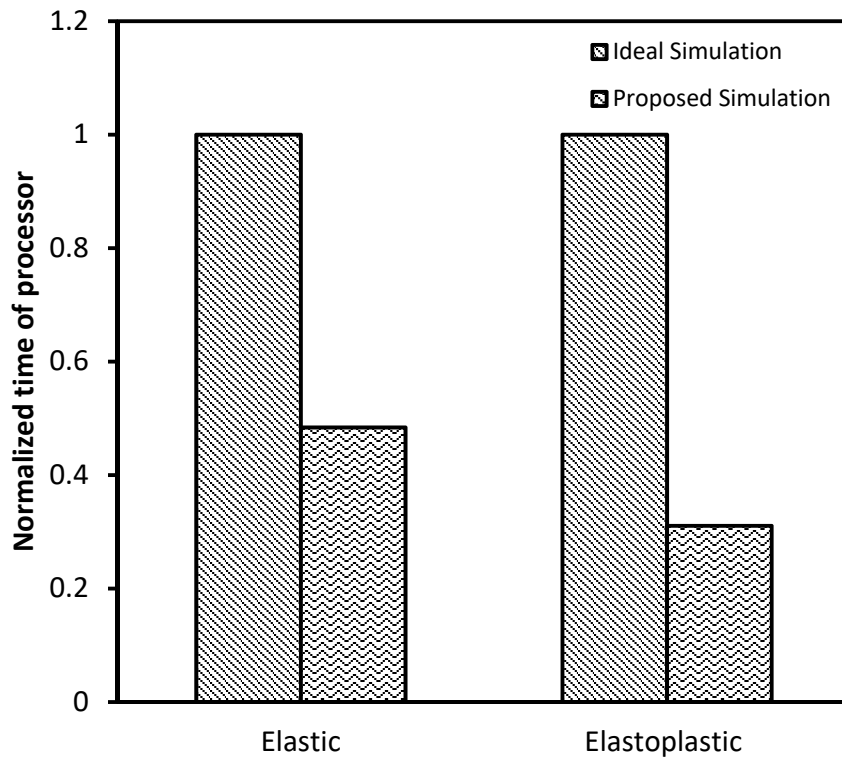
416

417

418

419

420



421

422

423

Figure 10: Effect of the proposed scheme on computational time, in comparison with the ideal simulation scheme